Stability Analysis of Underconstrained Cable-Driven Parallel Robots

Marco Carricato and Jean-Pierre Merlet

***Abstract*—This paper studies cable-driven parallel robots with less than six cables, in crane configuration. A geometrico-static model is provided, and the stability of static equilibrium is assessed within the framework of a constrained optimization problem. The method relies on ordinary linear-algebra routines, and it may be very simply applied to the most general architectures. Several examples are provided, concerning robots with a number of cables that range from 2 to 4.**

***Index Terms*—Cable-driven parallel robots (CDPRs), kinematic analysis, stability analysis, static analysis, underconstrained robots.**

I. Introduction

Cable-driven parallel robots (CDPRs) employ cables in place of rigid-body extensible legs to control the end-effector pose. CDPRs strengthen classic advantages characterizing closed-chain architectures versus serial ones, such as reduced masses and inertias, a larger payload to robot weight ratio, high dynamic performances, etc., while providing peculiar advantages, such as a larger workspace, reduced manufacturing and maintenance costs, ease of assembly and disassembly, superior modularity, and reconfigurability.

A CDPR intended to control the total number f of degrees of freedom (dof) of the end effector, i.e., a *fully constrained* robot, should have at least $f+1$ cables [1]. Indeed, since cables may exert only tensile axial forces, a redundancy of control actions is necessary to prevent cables from becoming slack [2]–[5]. The number of cables may be reduced to f if the end effector is linked to a constraining mechanism [6], [7] or it is submitted to an external force of convenient magnitude and direction that steadily acts upon it. One example of the latter case is provided by crane-type manipulators [8], [9], in which gravity plays the role of an additional virtual cable. A rich literature exists for fully constrained robots, as they have attracted much interest from the research community [1]–[19].

This paper studies *underconstrained* CDPRs, which are equipped with a number of cables n smaller than f, thus allowing only n dofs of the end effector to be controlled. CDPRs with a limited number of cables may be used in several applications (such as measurement, rescue, service or rehabilitation operations [20]–[24]), in which the task to be performed requires a limited number of controlled freedoms or a limitation of dexterity is acceptable in order to decrease complexity, cost, set-up time, likelihood of cable interference, etc. Compared with fully constrained manipulators, limited research has been conducted on underconstrained CDPRs [25]–[31].

Manuscript received February 13, 2012; revised June 12, 2012; accepted August 29, 2012. Date of publication September 28, 2012; date of current version February 1, 2013. This paper was recommended for publication by Associate Editor T. Murphey and Editor W. K. Chung upon evaluation of the reviewers' comments. This paper was presented in part at the 12th International Symposium on Advances in Robot Kinematics, Piran-Portorož, Slovenia, June 27–July 1, 2010.

M. Carricato is with the Department of Mechanical Engineering (DIEM) and the Center for Health Sciences and Technologies (HST-ICIR), University of Bologna, 40136 Bologna, Italy (e-mail: marco.carricato@unibo.it).

J.-P. Merlet is with the COPRIN Research Team, INRIA, Sophia Antipolis, BP 93, 06902 Sophia Antipolis Cedex, France (e-mail: jean-pierre.merlet@sophia.inria.fr).

Digital Object Identifier 10.1109/TRO.2012.2217795

A major challenge in the kinematic study of underconstrained CDPRs comes from the fact that, when the actuators are locked and cable lengths are assigned, the end effector is still movable so that the actual configuration is determined by the applied forces. Accordingly, *loop-closure* and *mechanical-equilibrium equations* must be simultaneously solved, and displacement-analysis problems become, more properly speaking, *geometrico-static*. As the end-effector pose depends on the applied load, it may change due to external disturbances so that investigating equilibrium stability is essential. An equilibrium configuration is actually *feasible* only if *cable tensions are positive* and *equilibrium is stable*.

In this paper, underconstrained n–n CDPRs are considered, i.e., manipulators in which a fixed base and a mobile platform are connected to each other by n cables, with $n \leq 5$. The notation n–n denotes the number of *distinct* cable exit points on the base and anchor points on the platform. Cables are treated as inextensible and massless, and the platform is acted upon by a constant force, e.g., gravity. A geometrico-static model is presented, and inverse and direct geometrico-static problems are described. A general and efficient algorithm to assess the stability of equilibrium is proposed. The algorithm, which is based on a constrained optimization formulation, relies on ordinary linear-algebra routines, and it may be very simply applied to the most general architectures.

A CDPR with two cables is studied in detail to show the effectiveness of the proposed approach. Only *planar* models are available so far in the literature for this robot (cf., [26], [28], and [30]), but they do not provide the entire set of equilibrium configurations and they may cause unstable configurations to be inadvertently addressed as stable. The complex *spatial* behavior of the robot is described, and complete static and stability analyses are presented. To show the generality of the stability algorithm, this is also applied to exemplifying robots with three and four cables.

In all numerical examples that are presented in the text, measurements are expressed in SI units, with angles being computed in radians.

II. Geometrico-Static Model

Fig. 1 shows the model of an underconstrained n–n CDPR, for the case $n=3$. The ith cable ($i=1,\ldots,n$) exits from the fixed base at point A_i, and it is connected to the mobile platform at point B_i. The cable length is ρ_i, with $\rho_i > 0$. $Oxyz$ is a Cartesian coordinate frame that is fixed to the base, with $\mathbf{i}$, $\mathbf{j}$, and $\mathbf{k}$ being unit vectors along the coordinate axes. $Gx'y'z'$ is a Cartesian frame that is attached to the end effector. Without loss of generality, O is chosen to coincide with A_1. The platform pose is described by $\mathbf{X} = [\mathbf{x}; \mathbf{\Phi}]$, where $\mathbf{x}$ is the position vector of G in the fixed frame, and $\mathbf{\Phi}$ is the array grouping the variables parameterizing the platform orientation with respect to $Oxyz$. For the sake of brevity, the following symbols are also introduced:

$$\mathbf{a}_i = A_i - O, \quad \mathbf{r}_i = B_i - G, \quad \mathbf{s}_i = B_i - A_i$$

where

$$\mathbf{s}_i = \mathbf{x} + \mathbf{r}_i - \mathbf{a}_i. \tag{1}$$

The platform is acted upon by a constant force, e.g., gravity, which is assumed to be oriented as $\mathbf{k}$ and applied at G, without loss of generality. This force may be described by a 0-pitch wrench $Q\mathcal{L}_e$, where Q is the intensity of the force, and $\mathcal{L}_e$ is the normalized Plücker vector of the force line of action. The normalized Plücker vector of the line that is associated with the ith cable is $\mathcal{L}_i/\rho_i$, where, in axis coordinates,

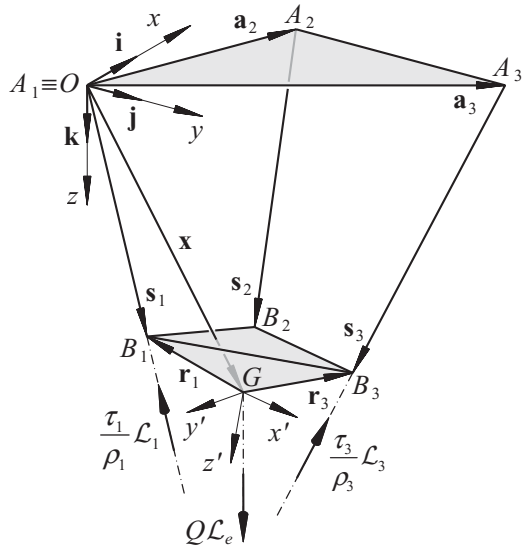

Fig. 1. Geometric model of a CDPR with three cables.

$\mathcal{L}_i = -[\mathbf{s}_i; \mathbf{p}_i \times \mathbf{s}_i]$, and $\mathbf{p}_i$ is any vector from an arbitrarily chosen reference point (called for brevity *moment pole*) to the cable line. Accordingly, the wrench exerted by the ith cable on the platform is $(\tau_i/\rho_i)\,\mathcal{L}_i$, with τ_i being a positive scalar that represents the intensity of the cable tensile force.

When all cables of the robots are *active* (i.e., taut), the set $\mathcal{C}$ of geometrical constraints imposed on the platform is made up by n equations, i.e.,

$$\|\mathbf{s}_i\|^2 = \rho_i^2, \quad i = 1, \ldots, n. \tag{2}$$

Since only n geometrical restraints are enforced, the platform preserves $6-n$ dofs, with its posture being determined by equilibrium laws, namely

$$\underbrace{[\,\mathcal{L}_1 \quad \cdots \quad \mathcal{L}_n \quad \mathcal{L}_e\,]}_{\mathbf{M}} \begin{bmatrix} (\tau_1/\rho_1) \\ \vdots \\ (\tau_n/\rho_n) \\ Q \end{bmatrix} = \mathbf{0} \tag{3}$$

where $\mathbf{M}$ is a $6 \times (n+1)$ matrix that only depends on the platform pose $\mathbf{X}$, and

$$\tau_i \geq 0, \quad i = 1, \ldots, n. \tag{4}$$

Equations (2) and (3) amount to $6+n$ scalar relations that involve $6+2n$ variables, namely the cable tensions and lengths, and the variables parameterizing the platform pose. Depending on the variables designated as input, one may tackle an *inverse geometrico-static problem* (IGP), if n variables concerning the platform pose are assigned, or a *direct* one (DGP), if cable lengths are given. In both cases, a square system of $6+n$ equations in $6+n$ unknowns is obtained so that a finite set of solutions is, in general, expected.

Both the IGP and the DGP may be simplified by eliminating cable tensions from the unknowns. Indeed, it emerges from (3) that equilibrium is possible only if

$$\text{rank}(\mathbf{M}) \leq n \tag{5}$$

to wit, if all $(n+1) \times (n+1)$ minors of $\mathbf{M}$ vanish. This strategy allows a large set of linearly independent relations that comprise neither the cable tensions nor the cable lengths to be obtained, a set that may be further enlarged by changing the moment pole with respect to which $\mathbf{M}$ is formulated and by canceling the corresponding minors. The mentioned strategy is particularly favorable, since the wealth of relationships in $\mathbf{X}$ replacing the static constraints may play a crucial role for the development of effective solution strategies for both the IGP and the DGP [32]–[37].

The IGP takes particular advantage of the partial decoupling of the system equations, since, in this case, the $6-n$ configuration variables that are needed to fully determine the platform pose may be directly computed by way of (a minimum of) $6-n$ relations that emerge from (5). Cable lengths may be subsequently computed by (2), and cable tensions may be obtained by a suitable set of linear independent relations chosen within (3).

The DGP poses more complex mathematical problems than the IGP, since in this case the platform configuration must be determined by simultaneously solving both the relations emerging from (5) and the n relations in (2). Furthermore, when cable lengths are assigned as inputs, nothing ensures, *a priori*, that when the platform reaches its stable equilibrium all cables are under tension. Accordingly, the final pose may be a DGP solution for *either* the current n–n CDPR *or* any m–m CDPR that may be derived from the initial n–n robot (with $m < n$). It follows that the overall solution set emerges by solving the DGP for all $\sum_{h=0}^{n-1} \binom{n}{n-h}$ CDPRs that may be obtained from the initial n–n robot.

III. Stability Analysis

Let an equilibrium configuration $\left(\bar{\mathbf{X}}, \bar{\rho}_1, \ldots, \bar{\rho}_m\right)$ be considered, with m being the number of *active* constraints (i.e., the number of cables contributing to supporting the platform). By a convenient reordering of indexes, taut cables may be assumed to be the first m, with $m \leq n$. Since the platform preserves $6-m$ dofs, it may displace under the effect of a transitory change in the external force acting on it, while cable lengths remain unvaried (for the sake of simplicity, it is assumed that the number of cables in tension does not change because of the perturbation, which is reasonable, but not necessarily true). The problem of assessing equilibrium stability is, thus, in order. In particular, while constraints (2) hold for $i = 1, \ldots, m$, G may generally move within a closed region of $\mathbb{R}^3$ (in some cases, a surface or a curve). If g is the frontier of this region, the equilibrium is stable any time the potential energy U associated with the external wrench, namely $-Q\mathbf{k} \cdot \mathbf{x}$, is at a *local minimum* on g. Loosely speaking, the platform is at rest at all points $\bar{G}$ of g in which the variety tangent to g is perpendicular to $\mathbf{k}$, with the equilibrium being stable if and only if a neighborhood $W_{\bar{G}}$ of $\bar{G}$ exists such that $\left(P - \bar{G}\right) \cdot \mathbf{k} < 0$, for all $P \in (g \cap W_{\bar{G}})$. Under such a condition, when the platform displaces under the effect of a perturbation, the original configuration is restored if the perturbation ceases. Finding the minima of a constrained function is a classic issue in optimization theory. An efficient algorithmic formalization is presented hereafter.

At equilibrium, the variation of the total potential energy of the platform due to a virtual displacement must be zero [38]. Such a variation is the opposite of the virtual work carried out by all forces that act on the platform, namely

$$\delta L = -Q\mathbf{k} \cdot \delta G + \sum_{i=1}^{m} \tau_i \frac{\mathbf{s}_i}{\rho_i} \cdot \delta B_i = 0. \tag{6}$$

If $\delta\mathbf{x}$ and $\delta\boldsymbol{\Theta}$ are, respectively, the virtual displacement of G and the virtual rotation of the platform, then

$$\delta G = \delta\mathbf{x}, \quad \delta B_i = \delta\mathbf{s}_i = \delta\mathbf{x} + \delta\boldsymbol{\Theta} \times \mathbf{r}_i \tag{7}$$

and thus

$$\delta L = -Q\mathbf{k} \cdot \delta\mathbf{x} + \sum_{i=1}^{m} \tau_i \frac{\mathbf{s}_i}{\rho_i} \cdot \delta\mathbf{s}_i = \mathbf{f} \cdot \delta\mathbf{x} + \mathbf{m} \cdot \delta\boldsymbol{\Theta} = 0 \tag{8}$$

where

$$\mathbf{f} = -Q\mathbf{k} + \sum_{i=1}^{m} \tau_i \frac{\mathbf{s}_i}{\rho_i}, \quad \mathbf{m} = \sum_{i=1}^{m} \tau_i \mathbf{r}_i \times \frac{\mathbf{s}_i}{\rho_i}. \tag{9}$$

Equation (8), from which $\mathbf{f}$ and $\mathbf{m}$ are inferred to be zero, is clearly equivalent, for $n = m$, to (3).

Since, for $\rho_i = \bar{\rho}_i$

$$\delta\left(\|\mathbf{s}_i\| - \rho_i\right) = \delta\|\mathbf{s}_i\| = \frac{\mathbf{s}_i \cdot \delta\mathbf{s}_i}{\rho_i} = \frac{\mathbf{s}_i \cdot \delta\mathbf{x} + \mathbf{r}_i \times \mathbf{s}_i \cdot \delta\boldsymbol{\Theta}}{\rho_i} \tag{10}$$

δL may be also written as

$$\delta L = -Q\mathbf{k} \cdot \delta\mathbf{x} + \sum_{i=1}^{m} \tau_i \delta\left(\|\mathbf{s}_i\| - \rho_i\right) \tag{11}$$

i.e., as the virtual variation of the Lagrange function[1]

$$L = -Q\mathbf{k} \cdot \mathbf{x} + \sum_{i=1}^{m} \tau_i \left(\|\mathbf{s}_i\| - \rho_i\right) \tag{12}$$

which shows that *Lagrange multipliers coincide with the cable tensions*, namely with the forces necessary to impose the geometrical constraints [38]. Such an observation is useful, since it allows the stability characteristics of the equilibrium to be assessed by evaluating the definiteness of the reduced Hessian $\mathbf{H}_r$ of L, i.e., the Hessian of L taken with respect to the configuration variables further restricted to the tangent space of the constraints $\mathcal{C}$ in (2) [39]. An algebraic expression of $\mathbf{H}_r$ is derived hereafter.

The second-order variation of δL is given by

$$\delta^2 L = -Q\mathbf{k} \cdot \delta^2\mathbf{x} + \sum_{i=1}^{m} \tau_i \frac{\delta\mathbf{s}_i \cdot \delta\mathbf{s}_i}{\rho_i} + \sum_{i=1}^{m} \tau_i \frac{\mathbf{s}_i \cdot \delta^2\mathbf{s}_i}{\rho_i} \tag{13}$$

with

$$\delta^2\mathbf{s}_i = \delta^2\mathbf{x} + \delta^2\boldsymbol{\Theta} \times \mathbf{r}_i + \delta\boldsymbol{\Theta} \times \left(\delta\boldsymbol{\Theta} \times \mathbf{r}_i\right). \tag{14}$$

Substituting (14) into (13) and enforcing $\mathbf{f} = \mathbf{m} = \mathbf{0}$ yields

$$\delta^2 L = \sum_{i=1}^{m} \frac{\tau_i}{\rho_i} \left[\delta\mathbf{s}_i \cdot \delta\mathbf{s}_i + \mathbf{s}_i \cdot \delta\boldsymbol{\Theta} \times \left(\delta\boldsymbol{\Theta} \times \mathbf{r}_i\right)\right] \tag{15}$$

and thus

$$\delta^2 L = \sum_{i=1}^{m} \frac{\tau_i}{\rho_i} \left\{ \delta\mathbf{x} \cdot \delta\mathbf{x} - 2\delta\mathbf{x} \cdot \left(\mathbf{r}_i \times \delta\boldsymbol{\Theta}\right) - \left(\mathbf{r}_i \times \delta\boldsymbol{\Theta}\right) \cdot \left[\left(\mathbf{x} - \mathbf{a}_i\right) \times \delta\boldsymbol{\Theta}\right] \right\} \tag{16}$$

[1]Equation (6) plus the relations $\{\tau_i > 0, \|\mathbf{s}_i\| = \rho_i\}$ for $i = 1, \ldots, m$ and $\{\tau_i = 0, \|\mathbf{s}_i\| < \rho_i\}$ for $i = m+1, \ldots, n$ is equivalent to the Karush–Kuhn–Tucker conditions for the minimization of L, provided that $\mathcal{L}_1, \ldots, \mathcal{L}_m$ are linearly independent.

or, in matrix notation

$$\delta^2 L = \sum_{i=1}^{m} \frac{\tau_i}{\rho_i} \left[\delta\mathbf{x}^T \delta\mathbf{x} - 2\delta\mathbf{x}^T \tilde{\mathbf{r}}_i \delta\boldsymbol{\Theta} + \delta\boldsymbol{\Theta}^T \tilde{\mathbf{r}}_i \left(\tilde{\mathbf{x}} - \tilde{\mathbf{a}}_i\right) \delta\boldsymbol{\Theta}\right] \tag{17}$$

where, for a generic vector $\mathbf{n}$, $\tilde{\mathbf{n}}$ denotes the skew-symmetric matrix that is associated with the operator $\mathbf{n}\times$.

$\delta^2 L$ is a bilinear form in the twist space of the platform. If the platform virtual displacement is expressed, in ray coordinates, as $\delta\mathbf{t} = [\delta\mathbf{x}; \delta\boldsymbol{\Theta}]$ and $\mathbf{I}_3$ denotes the 3×3 identity matrix, the symmetric matrix that is associated with this form is

$$\mathbf{H} = \sum_{i=1}^{m} \frac{\tau_i}{\rho_i} \begin{bmatrix} \mathbf{I_3} & -\tilde{\mathbf{r}}_i \\ \tilde{\mathbf{r}}_i & \frac{1}{2}\left[\tilde{\mathbf{r}}_i \left(\tilde{\mathbf{x}} - \tilde{\mathbf{a}}_i\right) + \left(\tilde{\mathbf{x}} - \tilde{\mathbf{a}}_i\right) \tilde{\mathbf{r}}_i\right] \end{bmatrix} \tag{18}$$

which represents the pseudo-Hessian of L ($\mathbf{H}$ is not a true and proper Hessian, since $\delta\boldsymbol{\Theta}$ is not generally integrable).

The tangent space of $\mathcal{C}$ is obtained by setting (10) equal to zero for all values of i. In matrix notation, this amounts to

$$\mathbf{J}\delta\mathbf{t} = \begin{bmatrix} \mathbf{s}_1^{\mathbf{T}} & \left(\mathbf{r}_1 \times \mathbf{s}_1\right)^T \\ \vdots & \vdots \\ \mathbf{s}_m^T & \left(\mathbf{r}_m \times \mathbf{s}_m\right)^T \end{bmatrix} \begin{bmatrix} \delta\mathbf{x} \\ \delta\boldsymbol{\Theta} \end{bmatrix} = \mathbf{0} \tag{19}$$

where the ith row of $\mathbf{J}$ coincides with $-\mathcal{L}_i$, expressed in axis coordinates and assuming G as the moment pole. $\mathbf{J}$ is the pseudo-Jacobian of the constraint equations.

If $\mathbf{N}$ is any $6 \times (6-m)$ matrix whose columns generate the null space of $\mathbf{J}$, the reduced Hessian of $\mathcal{C}$ is the following $(6-m) \times (6-m)$ matrix:

$$\mathbf{H}_r = \mathbf{N}^T \mathbf{H} \mathbf{N}. \tag{20}$$

A sufficient condition for the equilibrium to be stable consists in $\mathbf{H}_r$ being positive definite.

It is worth remarking that if $\mathbf{E}_3$ is the matrix such that $\delta\boldsymbol{\Theta} = \mathbf{E}_3 \delta\boldsymbol{\Phi}$, the Hessian and the Jacobian derived by differentiating L and $\mathcal{C}$ with respect to $\mathbf{x}$ and $\boldsymbol{\Phi}$ are equal, respectively, to $\mathbf{H}' = \mathbf{E}_6^T \mathbf{H} \mathbf{E}_6$ and $\mathbf{J}' = \mathbf{J}\mathbf{E}_6$, where $\mathbf{E}_6 = [\mathbf{I}_3, \mathbf{0}_3; \mathbf{0}_3, \mathbf{E}_3]$, and $\mathbf{0}_3$ is the 3×3 zero matrix. If the null space of $\mathbf{J}'$ is generated by $\mathbf{N}' = \mathbf{E}_6^{-1}\mathbf{N}$, then $\mathbf{H}_r = \mathbf{N}^T \mathbf{H} \mathbf{N} = \mathbf{N}'^T \mathbf{H}' \mathbf{N}'$.

The method that is proposed in [28] differs from the one presented here in that it determines the stability of equilibrium by looking at the Hessian of an *unconstrained* potential, explicitly expressed as a function of a number of independent coordinates equal to the number of taut cables. Such a mapping is, generally, difficult to obtain, and it requires extensive differential symbolic computation. Indeed, Michael *et al.* [28] apply important simplifications on the geometry of the robot. Instead, the method described here is based on a purely algebraic formulation (no differentiation is needed), and it may be very simply applied to the most general cases. No simplification of the robot geometry is necessary, and equilibrium stability may be assessed by ordinary linear-algebra routines (the order of magnitude of the computation time required to determine $\mathbf{H}_r$ and its eigenvalues is the msec).

IV. Geometrico-Static Analysis of the Spatial 2–2 Cable-Driven Parallel Robot

In this section, the case $n = 2$ is discussed in detail. In spite of its relative simplicity, the spatial manipulator with two cables has the merit of revealing, without the burden of heavy mathematical computations, a number of issues that are of fundamental importance to obtain physical insight into the kinematics and statics of underconstrained CDPRs.

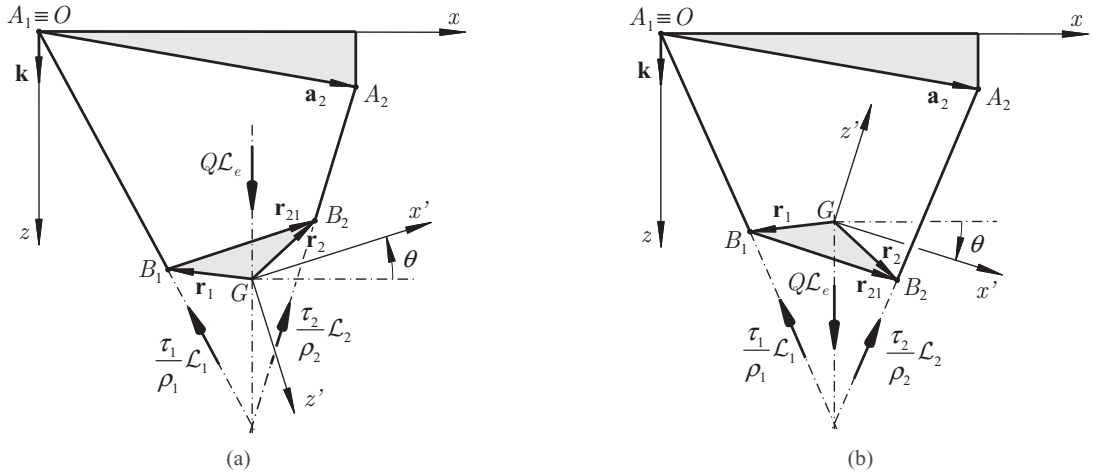

Fig. 2. Geometric model of a CDPR with two cables. (a) Operation mode I. (b) Operation mode II.

A. Modeling

Without loss of generality, the coordinate plane xz (which is parallel to $\mathbf{k}$) may be allowed to pass through A_1 and A_2, whereas $x'z'$ may be chosen so that it contains B_1, B_2, and G. For practical reasons, *the segment B_1B_2 is assumed to be strictly smaller than the projection of the segment A_1A_2 on the x-axis* (assumption A). This assumption is not conceptually necessary, but it rules out some special configurations, which could be handled with no difficulty, but whose analysis would burden the presentation. In particular, the possibility that both cables may be simultaneously parallel to $\mathbf{k}$ is discarded.

Since the cable wrenches and the external load represent pure forces, and three screws of equal pitch are linearly dependent if and only if they belong to a planar pencil [40], G, A_1, A_2, B_1, and B_2 must necessarily rest, at the equilibrium, in a plane parallel to $\mathbf{k}$. Accordingly, xz and $x'z'$ must be superimposed. If y and y' point in the same direction, the robot is said to work in operation mode I [see Fig. 2(a)] and the rotation matrix between $Oxyz$ and $Gx'y'z'$ is

$$\mathbf{R}_I = \begin{bmatrix} c_\theta & 0 & s_\theta \\ 0 & 1 & 0 \\ -s_\theta & 0 & c_\theta \end{bmatrix} \tag{21}$$

whereas if y and y' point in opposite directions, the robot is said to work in operation mode II [see Fig. 2(b)] and the rotation matrix is

$$\mathbf{R}_{II} = \begin{bmatrix} c_\theta & 0 & s_\theta \\ 0 & -1 & 0 \\ s_\theta & 0 & -c_\theta \end{bmatrix} \tag{22}$$

where θ is the angle formed by x' with x through a positive rotation around y', and s_θ and c_θ stand for $\sin\theta$ and $\cos\theta$, respectively. If $\mathbf{b}'_i$ is the coordinate vector of B_i in the $Gx'y'z'$ frame, then $\mathbf{r}_i = \mathbf{R}_I(\theta)\mathbf{b}'_i$ or $\mathbf{r}_i = \mathbf{R}_{II}(\theta)\mathbf{b}'_i$.

Distinguishing these *two operation* modes is important, since they provide *distinct* equilibrium configurations (and one set cannot be obtained from the other by planar movements). Indeed, when initially assembled, the CDPR moves to a pose corresponding to one operation mode. In general, after a displacement, the equilibrium pose still belongs to the same mode. However, when the robot is not constrained to move on a given plane by external means, appropriate changes in the cable lengths may bring the platform to an unstable equilibrium configuration, from which it may move away changing its operation mode (see Section IV-D).

If $O \equiv A_1$ is chosen as the moment pole, $\mathcal{L}_i$ and $\mathcal{L}_e$ may be, respectively, expressed as $-[\mathbf{s}_i;\ \mathbf{a}_i \times \mathbf{s}_i]$ and $[\mathbf{k};\ \mathbf{x} \times \mathbf{k}]$ so that the matrix $\mathbf{M}$ in (3) becomes

$$\mathbf{M} = \begin{bmatrix} -(\mathbf{x}+\mathbf{r}_1) & \mathbf{a}_2 - (\mathbf{x}+\mathbf{r}_2) & \mathbf{k} \\ \mathbf{0} & -\mathbf{a}_2 \times (\mathbf{x}+\mathbf{r}_2) & \mathbf{x} \times \mathbf{k} \end{bmatrix}. \tag{23}$$

Since at the equilibrium all vector components parallel to the y-axis and all moment components perpendicular to it are equal to zero, they may be ignored. Therefore, the matrix

$$\mathbf{M}' = \begin{bmatrix} \mathbf{x}+\mathbf{r}_1 & \mathbf{r}_{21} - \mathbf{a}_2 & \mathbf{k} \\ \mathbf{0} & \mathbf{a}_2 \times (\mathbf{x}+\mathbf{r}_2) & \mathbf{x} \times \mathbf{k} \end{bmatrix} \tag{24}$$

obtained from $\mathbf{M}$ by elementary column transformations and by setting $\mathbf{r}_{ij} = \mathbf{r}_i - \mathbf{r}_j$, $i \neq j$, may be condensed as

$$\mathbf{M}' = \begin{bmatrix} x + r_{1x} & r_{21x} - a_{2x} & 0 \\ z + r_{1z} & r_{21z} - a_{2z} & 1 \\ 0 & \mathbf{a}_2 \times (\mathbf{x}+\mathbf{r}_2) \cdot \mathbf{j} & -x \end{bmatrix}. \tag{25}$$

Under assumption A, $|r_{21x}| \leq \|\mathbf{r}_{21}\| < |a_{2x}| \neq 0$. Accordingly, it emerges from (25) that $\operatorname{rank} \mathbf{M}' \geq 2$ and (5) holds if and only if $\det \mathbf{M}' = 0$, namely

$$\begin{aligned} p_1 := {} & (r_{21x}x + a_{2x}r_{1x})\, z - r_{21z}x^2 \\ & + (r_{1z}r_{2x} - r_{1x}r_{2z} + a_{2x}r_{21z} - a_{2z}r_{2x})\, x \\ & + r_{1x}\,(a_{2x}r_{2z} - a_{2z}r_{2x}) = 0. \end{aligned} \tag{26}$$

Equation (26), which is equivalent to requiring $\mathcal{L}_1$, $\mathcal{L}_2$, and $\mathcal{L}_e$ to form a planar pencil, only depends on the variables x, z, and θ (through the components of $\mathbf{r}_{ij}$).

The two constraint equations that emerge from (2) may be linearly combined in the form

$$p_2 := x^2 + z^2 + 2\,(r_{1x}x + r_{1z}z) + \|\mathbf{r}_1\|^2 - \rho_1^2 = 0 \tag{27}$$

$$\begin{aligned} p_3 := {} & 2\,(a_{2x} - r_{21x})\, x + 2\,(a_{2z} - r_{21z})\, z \\ & + \|\mathbf{r}_1\|^2 - \|\mathbf{a}_2 - \mathbf{r}_2\|^2 + \rho_2^2 - \rho_1^2 = 0. \end{aligned} \tag{28}$$

They comprise the variables x, z, θ, ρ_1, and ρ_2.

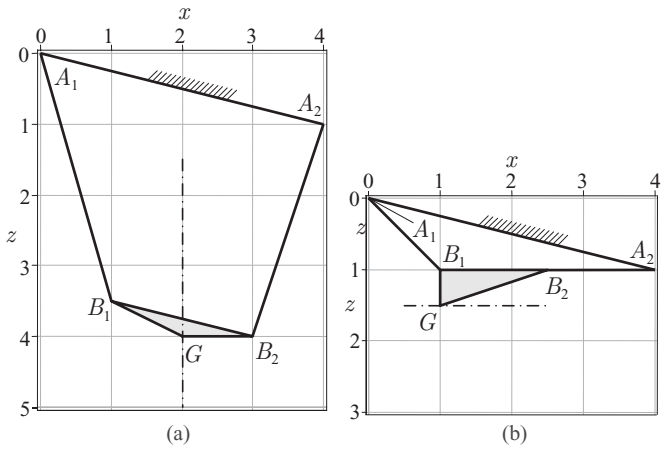

Fig. 3. Examples of one-dimensional solution sets of the IGP with assigned orientation for the 2–2 robot. (a) $a_{2x} = 4, a_{2z} = 1, r_{2x} = -r_{1x} = 1, r_{1z} = -0.5, r_{2z} = 0$, and $x = 2$. (b) $a_{2x} = 4, a_{2z} = 1, r_{1x} = 0, r_{2x} = 1.5, r_{2z} = r_{1z} = -0.5$, and $z = 1.5$. In both cases, equilibrium configurations are *feasible* along the entire path.

B. Inverse Geometrico-Static Problem

The IGP may be directly solved by (26). Different cases may be distinguished, depending on which pose parameters are assigned. In particular, when the orientation is known (including the operation mode and θ), one may assign either one component of $\mathbf{x}$ or an approximate global position of G.[2]

1) Orientation and Variable x Are Assigned: If the orientation and x are known, (26) provides a single solution in z, as long as $r_{21x}x \neq -a_{2x}r_{1x}$.

If the latter condition does not hold, the problem may be solved only if the entire polynomial vanishes, in which case the solution set is one-dimensional, and it coincides with a line that is parallel to $\mathbf{k}$. Under assumption A, this occurs if either one of the following conditions holds:

1) $r_{ix} = 0$ and $x = a_{ix}$, with $i = 1$ or 2;
2) $\mathbf{a}_2 \times \mathbf{r}_{21} \cdot \mathbf{j} = 0, r_{21x} \neq 0$ and $x = -a_{2x}r_{1x}/r_{21x}$.

In the former case, A_i, B_i, and G lie on a line parallel to $\mathbf{k}$, and the robot operates like a one-dof crane, with the ith cable holding the entire charge. In the latter case, the line segments A_1A_2 and B_1B_2 are parallel, and the platform may follow a quasi-static linear path parallel to $\mathbf{k}$, with orientation being constant and the load being sustained by both cables [see Fig. 3(a)].

2) Orientation and Variable z Are Assigned: If the orientation and z are assigned, (26) provides, in general, two solutions in x.

If all coefficients of p_1 vanish, the solution set is one-dimensional, and it coincides with a line perpendicular to $\mathbf{k}$. Under assumption A, p_1 is identically nought if $r_{1z} = r_{2z}, z + r_{1z} = a_{jz}$, and $r_{ix} = 0$, with $i \neq j$, namely if points B_1, B_2, and A_j lie on a line perpendicular to $\mathbf{k}$, and the segment B_iG is parallel to $\mathbf{k}$ [see Fig. 3(b)]. In this case, $\mathcal{L}_1, \mathcal{L}_2$, and $\mathcal{L}_e$ intersect in B_i.

3) Orientation and an Approximate Position of G Are Assigned: If the orientation and an approximate desired location (x_d, z_d) of G are assigned, x and z must be found so that (26) is satisfied and the error $\epsilon = (x - x_d)^2 + (z - z_d)^2$ is minimized. Since both ϵ and p_1 are continuously differentiable in x and z, the global minimum of ϵ is a stationary point of the function $L_\epsilon = (x - x_d)^2 + (z - z_d)^2 + \lambda p_1(x, z)$. Setting the derivatives of L_ϵ with respect to x and z to zero provides a linear system in x and z, by which x and z may be determined as functions of λ. Upon substituting $x = x(\lambda)$ and $z = z(\lambda)$ into p_1, a quartic polynomial in λ is obtained. Its real roots are the stationary points of L_ϵ, among which the global minimum may be determined by the evaluation of ϵ. Clearly, this optimal configuration is feasible only if the conditions concerning cable-tension signs and stability are satisfied.

4) Position Is Assigned: When $\mathbf{x}$ is assigned and the orientation is unknown, by letting $\mathbf{r}_i = \mathbf{R}_I(\theta)\mathbf{b}'_i$ or $\mathbf{r}_i = \mathbf{R}_{II}(\theta)\mathbf{b}'_i$ $(i = 1, 2)$, p_1 becomes a quadratic polynomial in s_θ and c_θ. For each operation mode, the resultant of p_1 and the trigonometric identity yields a quartic equation in s_θ. For each root in s_θ, (26) provides a single value of c_θ and thus of θ. The problem admits, altogether, eight solutions, all of which may be real. When $x = a_{ix}$, with $i = 1$ or 2, the algorithm provides, among its solutions, the configurations for which only the ith cable is taut.

C. Direct Geometrico-Static Problem

When the DGP is dealt with, ρ_1 and ρ_2 are assigned and the platform pose must be found. The operation mode is *a priori* unknown.

For each mode, (28) allows x to be expressed as a linear function of z, since p_3 is linear in x and z and the coefficient $2(a_{2x} - r_{21x})$ is different from zero under assumption A. Substituting $x = x(z)$ into p_1 and p_2 yields two quadratic equations in z, namely $p_4 = 0$ and $p_5 = 0$, from which z may be eliminated. By canceling out the nonzero factor $16\,(a_{2x} - r_{21x})^4$, a single equation in θ may be further obtained in the form $p_6 = 0$. By Weierstrass substitutions, s_θ and c_θ may be conveniently expressed as functions of $\tan(\theta/2)$, here denoted as t_θ. By clearing the factor $(1 + t_\theta^2)^6$, a 12th-degree polynomial equation in t_θ is finally obtained, i.e.,

$$\sum_{k=0}^{12} B_k t_\theta^k = 0. \tag{29}$$

For each solution of (29), a single value of z is computed by the greatest common divisor of p_4 and p_5. The existence of such a value is guaranteed [41], since the coefficient of the monomial z^2 of p_4 is $4\|\mathbf{a}_2 - \mathbf{r}_{21}\|^2$ and this number is nonzero under assumption A. A single value of x is finally obtained by (28). By considering both operation modes, the problem admits up to 24 solutions.

The solution of the DGP presented here is an improvement with respect to what was previously presented in the literature, as

1) a maximum of only 12 solutions is reported in [28] and [30], where only one operation mode is taken into account;
2) the solution set computed by the elimination procedure presented in [30] is not minimal, since it includes four spurious roots.

Equilibrium configurations that involve a single cable in tension may be searched for by setting, for each operation mode and for $i = 1$ and 2, $B_i = A_i + \rho_i\mathbf{k}, G = B_i \pm \|\mathbf{r}_i\|\mathbf{k}$, and $B_j = G + \mathbf{r}_j$, with $j \neq i$ [postures for which $B_i = A_i - \rho_i\mathbf{k}$ may be discarded, for they would not comply with the requirement (4)]. Provided that $\|\mathbf{s}_j\| \leq \rho_j$, these configurations are acceptable and they may be appended to the solution set emerging from (29).

It is apparent that

1) when B_1, B_2, and G are aligned, the two operation modes coincide;
2) when $a_{2z} = 0$, each operation mode may be obtained from the other by a reflection through the x-axis.

The total degree of (29) has an apparent geometrical interpretation [28]. If the platform is thought of as the coupler of a four-bar

[2]The constant-orientation statical workspace of the 2–2 CDPR is a conic on the xz-plane, as observed in [26].

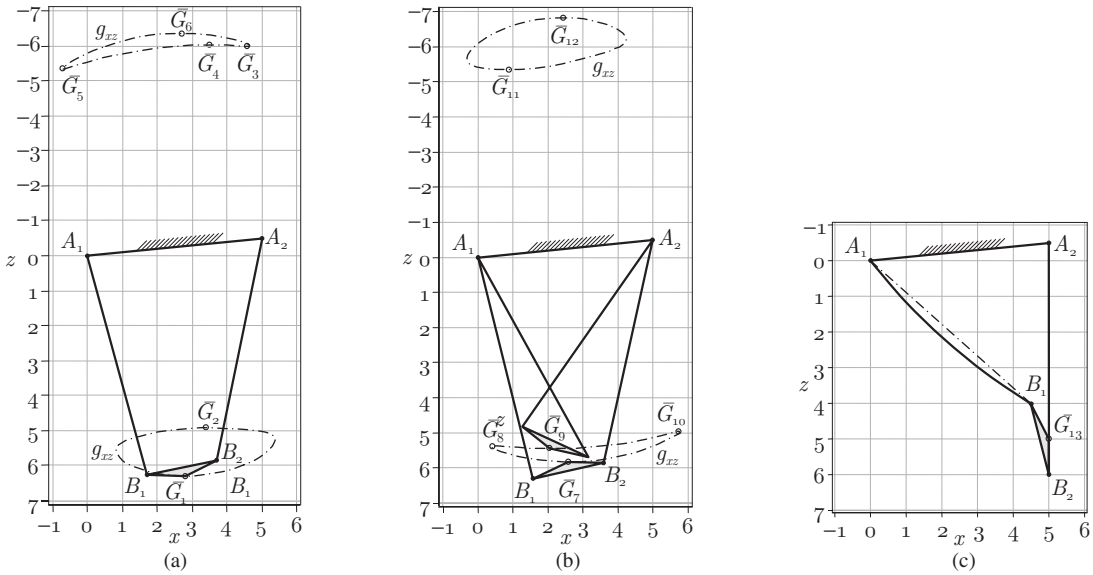

Fig. 4. Solution set of the DGP of a 2–2 robot with distinct operation modes such that $a_{2x} = 5, a_{2z} = -0.5, b'_{1x} = -1, b'_{1z} = -0.5, b'_{2x} = 1, b'_{2z} = 0, \rho_1 = \rho_2 = 6.5$, and $Q = 10$. There are six real potential equilibrium configurations in each mode [figures (a)–(b)] and one equilibrium configuration for which one cable is taut and the other is slack [figure (c), $\|B_1 - A_1\| = 6.02 < \rho_1$]. Only one equilibrium configuration is feasible [with $G \equiv \bar{G}_1$, figure (a)].

linkage whose grounded links are the cables (with assigned lengths), the locus g_{xz} of the positions that G may assume on the xz-plane under constraints (2) may be interpreted as a coupler curve, which is, in general, a sextic of class 12 [40]. Accordingly, there are up to 12 lines tangent to g_{xz} passing through the point at infinity perpendicular to $\mathbf{k}$. Since the equilibrium configurations are the points of g_{xz} in which the tangent line is perpendicular to $\mathbf{k}$ (see Section III), the maximum number of solutions of the DGP must be 12, for *each* operation mode.

D. Stability Analysis

If the robot is constrained to lie on the xz-plane by external means (e.g., it is suspended against a vertical wall with negligible friction), other than by equilibrium conditions, all vector components parallel to the y-axis and all moment components perpendicular to it may be neglected in stability analysis too, so that matrices $\mathbf{J}$ and $\mathbf{H}$ specialize as, respectively,

$$\mathbf{J} = \begin{bmatrix} (\mathbf{x} + \mathbf{r}_1)^T_{xz} & \mathbf{r}_1 \times \mathbf{x} \cdot \mathbf{j} \\ (\mathbf{x} + \mathbf{r}_2 - \mathbf{a}_2)^T_{xz} & \mathbf{r}_2 \times (\mathbf{x} - \mathbf{a}_2) \cdot \mathbf{j} \end{bmatrix} \tag{30}$$

and

$$\mathbf{H} = \sum_{i=1}^{2} \frac{\tau_i}{\rho_i} \begin{bmatrix} \mathbf{I_2} & -(\mathbf{r}_i \times \mathbf{j})_{xz} \\ -(\mathbf{r}_i \times \mathbf{j})^T_{xz} & -\mathbf{r}_i \times \mathbf{j} \cdot [(\mathbf{x} - \mathbf{a}_i) \times \mathbf{j}] \end{bmatrix}. \tag{31}$$

In this occurrence, the null space of $\mathbf{J}$ may be generated by the vector

$$\mathbf{N} = \begin{bmatrix} -\mathrm{adj}\,(\mathbf{J}_{12,12})\,\mathbf{J}_{12,3} \\ \det\,(\mathbf{J}_{12,12}) \end{bmatrix} \tag{32}$$

where adj denotes the adjugate matrix, and $\mathbf{J}_{ij,hk}$ denotes the block matrix obtained from rows i and j, and columns h and k, of $\mathbf{J}$. Accordingly, the reduced Hessian is a scalar, i.e., H_r.

However, stability assessment by way of (30)–(32) takes into account only the motions that occur on the xz-plane, and it is *not* able to provide correct information if the robot is free to move out of this plane, which is likely to occur in practice. In this case, stability must be assessed by way of the *tridimensional formulas* provided in Section III, with $\mathbf{J}$, $\mathbf{N}$, and $\mathbf{H}_r$ being, respectively, $2 \times 6, 6 \times 4$, and 4×4 matrices. This observation and the fact that the 2–2 CDPR is able to switch between distinct planar modes during its operation *prevent this robot from being considered as a planar mechanism*.

E. Examples

Two examples that concern the DGP and the stability analysis of the 2–2 CDPR are presented hereafter.

1) Example 1: An exemplifying robot with assigned cable lengths and distinct operation modes ($a_{2z} \neq 0$, and B_1, B_2, and G are not aligned) is represented in Fig. 4. Fig. 4(a) and Fig. 4(b) portray the loci g_{xz} for modes I and II, respectively. On each (bicursal) locus, the figure shows the equilibrium positions of G corresponding to the real solutions of (29). Fig. 4(c) depicts the unique valid equilibrium configuration for which a single cable is in tension.

Table I reports the corresponding values of the pose and cable tensions, as well as an indication about the definiteness of the "planar" and the "spatial" reduced Hessians (the symbols $>, \geq, <, \leq$, and $<>$ stand, respectively, for positive definite, positive semidefinite, negative definite, negative semidefinite, and indefinite).

The configurations for which cable tensions are nonnegative lie, naturally, in the half-plane $z > 0$. Among these, $H_r > 0$ in $\bar{G}_1, \bar{G}_7$, and $\bar{G}_9$. (Fig. 4(a) and Fig. 4(b) depict the robot configurations in such positions.) However, $\bar{G}_1, \bar{G}_7$, and $\bar{G}_9$ are local minima of the potential energy only if movements on the xz-plane are considered exclusively. If, instead, possible motions out of the xz-plane are taken into account, the analysis of $\mathbf{H}_r$ proves that the configurations centered in $\bar{G}_7$ and $\bar{G}_9$ are unstable. The platform may, in fact, move away from the former by tilting over the axis B_1B_2, whereas it may move away from the latter by rotating around an axis lying on the xz-plane, thus unfolding the cables away from the crossed configuration.

2) Example 2: When $a_{2z} = 0$ and B_1, B_2, and G are collinear, the loci g_{xz} of the two operation modes coincide and g_{xz} is a curve symmetric about the x-axis. Hence, for any equilibrium configuration in the half-plane $z > 0$, there is a symmetric one in the half-plane

TABLE I
REAL EQUILIBRIUM CONFIGURATIONS OF THE ROBOT SHOWN IN FIG. 4

Conf.	Mode	$\bar{G}$	θ	τ_1	τ_2	H_r	$\mathbf{H}_r$
1	I	$(+2.8195, +6.2996)$	0.4401	$+4.40$	$+5.87$	$>$	$>$
2	I	$(+3.3873, +4.9258)$	3.8030	$+4.07$	$+7.59$	$<$	$<>$
3	I	$(+4.5981, -5.9869)$	1.7064	-1.16	-9.15	$>$	$<>$
4	I	$(+3.5525, -6.0249)$	2.5414	-4.06	-7.31	$<$	$<>$
5	I	$(-0.6925, -5.3383)$	5.3535	-11.34	$+1.98$	$>$	$<>$
6	I	$(+2.7050, -6.3545)$	0.5098	-4.86	-5.42	$<$	$<>$
7	II	$(+2.5883, +5.8251)$	0.0197	$+4.85$	$+5.42$	$>$	$<>$
8	II	$(+0.4292, +5.3662)$	5.0410	$+9.10$	$+1.24$	$<$	$<>$
9	II	$(+2.0511, +5.4517)$	3.8193	$+6.38$	$+5.38$	$>$	$<>$
10	II	$(+5.7566, +4.9491)$	1.3750	-2.15	$+11.47$	$<$	$<>$
11	II	$(+0.8778, -5.3512)$	2.4941	-8.62	-2.41	$>$	$<>$
12	II	$(+2.4326, -6.8251)$	0.0169	-5.38	-4.89	$<$	$<$
13	-	$(+5.0000, +5.0000)$	$\pi/2$	$+0.00$	$+10.00$	$<$	$<>$

TABLE II
EQUILIBRIUM CONFIGURATIONS OF THE 2–2 ROBOT SHOWN IN FIG. 5

Conf.	$\bar{G}$	θ	τ_1	τ_2	H_r	$\mathbf{H}_r$
1	$(+2.50000, +6.32456)$	0	$+5.14$	$+5.14$	$>$	$\geq$
2	$(+0.91886, +5.47723)$	$2\pi/3$	$+8.36$	$+2.59$	$<$	$<>$
3	$(+1.56894, +5.47797)$	2.5410	$+7.38$	$+4.15$	$>$	$<>$
4	$(+2.50000, +5.47723)$	π	$+5.93$	$+5.93$	$<$	$<>$
5	$(+3.43106, +5.47797)$	3.7422	$+4.15$	$+7.38$	$>$	$<>$
6	$(+4.08114, +5.47723)$	$4\pi/3$	$+2.59$	$+8.36$	$<$	$<>$

$z < 0$. If, without loss of generality, the x'-axis is chosen so as to pass through B_1, B_2, and G (so that $b'_{1z} = b'_{2z} = 0$), the symmetry emerges analytically by the particular form of (29), since the coefficients of all odd-power monomials vanish. If, moreover, $b'_{1x} = -b'_{2x}$ and $\rho_1 = \rho_2$, the problem has four solutions at $x = a_{2x}/2$: two corresponding to $\theta = 0$ and two corresponding to $\theta = \pi$. Since the latter may not be accounted for by (29),[3] the leading coefficient of the polynomial at the left-hand side of (29) vanishes and its degree lowers to 10.

Fig. 5 shows a 2–2 robot of this kind, similar to an example reported in [28]. The geometric dimensions approximately respect the proportions of a Chebyshev straight-line linkage. In this case, *all* solutions of (29) are real. The coupler curve g_{xz} is bicursal, and it is symmetric with respect to the x-axis. Fig. 5 portrays the portion of g_{xz} that lies on the half-plane $z > 0$, together with the stationary configurations of G that lie on it. These are the only ones in which cable tensions are positive. Table II reports the corresponding numeric values of the pose and the cable tensions, as well as the definiteness of the "planar" and the "spatial" reduced Hessians. When only movements on the xz-plane are considered, the potential energy is at a minimum in $\bar{G}_1, \bar{G}_3$, and $\bar{G}_5$, and, accordingly, $H_r > 0$. Michael *et al.* [28] assess such postures (whose corresponding robot configurations are depicted in the figure) as stable. However, if all possible movements of the platform are taken into account, the analysis of $\mathbf{H}_r$ proves that the only stable configuration is that centered in $\bar{G}_1$.[4]

[3]Equation (29) is unable to provide $\theta = \pi$ as a solution, since, in this case, $t_\theta \to \infty$. This solution must be detected by direct evaluation of p_6.

[4]It must be said that, even in the "planar" case, the robustness of the poses in $\bar{G}_3$ and $\bar{G}_5$ to external disturbances is very small, since the differences in potential energy between the stationary configurations lying on the "rectilinear" part of g_{xz} are almost negligible.

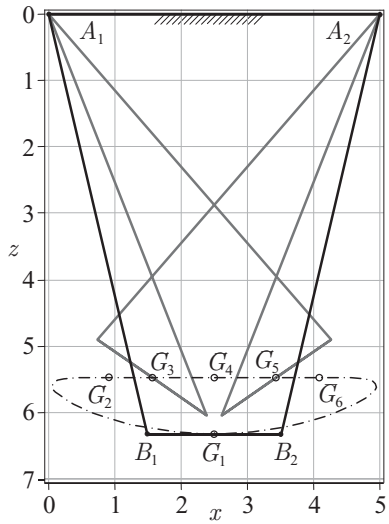

Fig. 5. Solution set of the DGP of a 2–2 robot with coincident operation modes such that $a_{2z} = b'_{1z} = b'_{2z} = 0, a_{2x} = 5, b'_{2x} = -b'_{1x} = 1, \rho_1 = \rho_2 = 6.5$, and $Q = 10$. There are 12 *real* potential equilibrium configurations, each one with multiplicity 2 (only those in the half-plane $z > 0$ are shown), and no equilibrium configurations with a single cable in tension. Only one equilibrium configuration is *feasible* (with $G \equiv \bar{G}_1$).

By assigning a small perturbation to the geometric parameters of the robot in Fig. 5 (by setting, for instance, $a_{2z} = b'_{2z} = \epsilon$ and $b'_{2x} = 1 + \epsilon$, with $\epsilon = 0.002$), the two operation modes may be separated, with all solutions in each mode being kept real. In this way, the DGP of the 2–2 robot is proven to have up to 24 *real* distinct solutions. Of course, this count only concerns *potential* solutions of the problem at hand, since it does not take into account the constraints imposed by the sign of cable tensions and the stability of equilibrium. Once such constraints are imposed and solutions are sifted, the number of *feasible* configurations is drastically reduced.

V. STABILITY ANALYSIS OF n–n CABLE-DRIVEN PARALLEL ROBOTS, WITH $n \geq 3$

The application of the stability algorithm presented in Section III to an n–n CDPR with a number m of taut cables greater than 2 presents no difficulty with respect to the case $m = 2$. Indeed, (18)–(20) hold for an arbitrary robot geometry and for any value of m comprised between 2 and 5. Actually, when m increases, the order of $\mathbf{N}$ and $\mathbf{H}_r$ lowers and the eigenproblem becomes simpler. In fact, for $m = 3$, 4, and 5, $\mathbf{H}_r$ has dimensions $3 \times 3, 2 \times 2$, and 1, respectively.

Tables III and IV report the real equilibrium configurations of two exemplifying robots with assigned cable lengths, with $n = 3$ and $n = 4$, respectively. For the sake of brevity, only the solutions with nonnegative tension in all cables are reported. The platform orientation is expressed in terms of Euler parameters. Equilibrium configurations are obtained by solving (2)–(3) via homotopy continuation. Details cannot be included here due to space limitation, but readers may find the complete derivation in [32], [35], and [36]. The stability of each configuration is assessed by computing the eigenvalues of $\mathbf{H}_r$. The 3–3 robot in Table III has six equilibrium configurations with all cables in tension, with only the first one being stable. There are no equilibrium configurations with slack cables. The 4–4 robot in Table IV has two equilibrium configurations with all cables active and one configuration in which two cables are slack. Interestingly, only the latter is stable.

TABLE III
STABILITY ANALYSIS OF A 3–3 ROBOT WITH $\mathbf{a}_2 = [10; 0; 0], \mathbf{a}_3 = [0; 12; 0], \mathbf{b}'_1 = [1; 0; 0], \mathbf{b}'_2 = [0; 1; 0], \mathbf{b}'_3 = [0; 0; 1], (\rho_1, \rho_2, \rho_3) = (7.5, 10, 9.5)$

Conf.	(e_0, e_1, e_2, e_3)	(x, y, z)	Q	(τ_1, τ_2, τ_3)	$\mathbf{H}_r$
1	$1, -3.355398, +0.542536, +1.711023$	$2.931333, 4.076890, 6.045191$	10	$5.26, 5.11, 5.81$	$>$
2	$1, -4.222022, -5.904163, -0.471928$	$1.680460, 3.574305, 5.560548$	10	$6.84, 3.05, 6.14$	$<>$
3	$1, -1.165850, -1.273125, -1.006600$	$1.399261, 3.279485, 5.531283$	10	$6.76, 2.51, 4.86$	$<>$
4	$1, -0.548350, -0.487719, -1.210596$	$1.815931, 4.302219, 5.551637$	10	$5.46, 3.25, 5.50$	$<>$
5	$1, -0.504474, +2.590310, -1.247955$	$3.523134, 5.532024, 5.262678$	10	$2.89, 7.87, 9.12$	$<>$
6	$1, +0.543433, -0.145506, +0.569622$	$3.024095, 4.730974, 3.301921$	10	$5.90, 7.83, 9.56$	$<$

TABLE IV
STABILITY ANALYSIS OF A 4–4 ROBOT WITH
$\mathbf{a}_2 = [9; 0; 1], \mathbf{a}_3 = [11; 9; 0], \mathbf{a}_4 = [-2; 8; -1], \mathbf{b}'_1 = [-2; -1; -1], \mathbf{b}'_2 = [1; -2; 0], \mathbf{b}'_3 = [2; 1; -1], \mathbf{b}'_4 = [0; 2; -1], (\rho_1, \rho_2, \rho_3, \rho_4) = (6, 7, 8, 9)$

Conf.	(e_0, e_1, e_2, e_3)	(x, y, z)	Q	$(\tau_1, \tau_2, \tau_3, \tau_4)$	$\mathbf{H}_r$
1	$1, -7.844289, -19.344432, +2.218428$	$4.566026, 3.268288, 0.837539$	10	$12.52, 15.42, 9.38, 12.36$	$<>$
2	$1, -24.730185, +0.758067, -1.956189$	$4.468110, 4.167902, 0.975350$	10	$8.38, 11.17, 11.33, 12.92$	$<>$
3	$1, +0.035015, -0.054068, +0.111500$	$4.517492, 3.696130, 5.963458$	10	$7.54, 0.00, 6.25, 0.00$	$>$

VI. CONCLUSION

This paper has studied underconstrained CDPRs with less than six cables, in crane configuration. In such robots, kinematics and statics are intrinsically coupled, and they must be solved simultaneously.

An algorithm based on a constrained optimization formulation was provided to assess the equilibrium stability. The algorithm relies on linear-algebra routines, and it may be very simply applied to the most general architectures, both planar and spatial. This is a significant improvement with respect to what is proposed in the literature for similar cases.

A robot with two cables was studied in detail. The inverse and the direct geometrico-static problems were worked out, and the complete solution sets were obtained. Particular emphasis was placed on equilibrium stability. The example showed that, even in the simplest case, the geometrico-static problems of underconstrained CDPRs gain appreciable complexity with respect to analogous tasks concerning rigid-link mechanisms and tricky issues may emerge. Indeed, some of the presented results emended previous literature on the topic.

The generality of the stability algorithm proposed in this paper was finally proven by two examples concerning robots with three and four cables.

REFERENCES

[1] R. G. Roberts, T. Graham, and T. Lippitt, "On the inverse kinematics, statics, and fault tolerance of cable-suspended robots," *J. Robot. Syst.*, vol. 15, no. 10, pp. 581–597, 1998.

[2] S. Kawamura, H. Kino, and C. Won, "High-speed manipulation by using parallel wire-driven robots," *Robotica*, vol. 18, no. 1, pp. 13–21, 2000.

[3] S. Tadokoro, Y. Murao, M. Hiller, R. Murata, H. Kohkawa, and T. Matsushima, "A motion base with 6-DOF by parallel cable drive architecture," *IEEE/ASME Trans. Mechatronics*, vol. 7, no. 2, pp. 115–123, Jun. 2002.

[4] M. Hiller, S. Fang, S. Mielczarek, R. Verhoeven, and D. Franitza, "Design, analysis and realization of tendon-based parallel manipulators," *Mech. Mach. Theory*, vol. 40, no. 4, pp. 429–445, 2005.

[5] A. Alikhani, S. Behzadipour, S. A. S. Vanini, and A. Alasty, "Workspace analysis of a three DOF cable-driven mechanism," *ASME J. Mech. Robot.*, vol. 1, no. 4, pp. 041005/1–7, 2009.

[6] S. E. Landsberger, "Design and construction of a cable-controlled, parallel link manipulator," Master's thesis, Dept. Mech. Eng., Mass. Inst. Technol., Cambridge, MA, 1984.

[7] S. Behzadipour and A. Khajepour, "A new cable-based parallel robot with three degrees of freedom," *Multibody Syst. Dyn.*, vol. 13, no. 4, pp. 371–383, 2005.

[8] J. Albus, R. Bostelman, and N. Dagalakis, "The NIST robocrane," *J. Robot. Syst.*, vol. 10, no. 5, pp. 709–724, 1993.

[9] Y. X. Su, B. Y. Duan, R. D. Nan, and B. Peng, "Development of a large parallel-cable manipulator for the feed-supporting system of a next-generation large radio telescope," *J. Robot. Syst.*, vol. 18, no. 11, pp. 633–643, 2001.

[10] M. Gouttefarde and C. M. Gosselin, "Analysis of the wrench-closure workspace of planar parallel cable-driven mechanisms," *IEEE Trans. Robot.*, vol. 22, no. 3, pp. 434–445, 2006.

[11] P. Bosscher, A. T. Riechel, and I. Ebert-Uphoff, "Wrench-feasible workspace generation for cable-driven robots," *IEEE Trans. Robot.*, vol. 22, no. 5, pp. 890–902, 2006.

[12] K. Kozak, Q. Zhou, and J. Wang, "Static analysis of cable-driven manipulators with non-negligible cable mass," *IEEE Trans. Robot.*, vol. 22, no. 3, pp. 425–433, Jun. 2006.

[13] S. Behzadipour and A. Khajepour, "Stiffness of cable-based parallel manipulators with application to stability analysis," *ASME J. Mech. Des.*, vol. 128, no. 1, pp. 303–310, 2006.

[14] E. Stump and V. Kumar, "Workspaces of cable-actuated parallel manipulators," *ASME J. Mech. Des.*, vol. 128, no. 1, pp. 159–167, 2006.

[15] X. Diao and O. Ma, "Vibration analysis of cable-driven parallel manipulators," *Multibody Syst. Dyn.*, vol. 21, no. 4, pp. 347–360, 2009.

[16] S. Bouchard, C. Gosselin, and B. Moore, "On the ability of a cable-driven robot to generate a prescribed set of wrenches," *ASME J. Mech. Robot.*, vol. 2, no. 1, pp. 011010/1–10, 2010.

[17] M. Gouttefarde, D. Daney, and J.-P. Merlet, "Interval-analysis-based determination of the wrench-feasible workspace of parallel cable-driven robots," *IEEE Trans. Robot.*, vol. 27, no. 1, pp. 1–13, Feb. 2011.

[18] D. Lau, D. Oetomo, and S. Halgamuge, "Wrench-closure workspace generation for cable driven parallel manipulators using a hybrid analytical-numerical approach," *ASME J. Mech. Des.*, vol. 133, no. 7, pp. 071004/1–10, 2011.

[19] G. Rosati, D. Zanotto, and S. K. Agrawal, "On the design of adaptive cable-driven systems," *ASME J. Mech. Robot.*, vol. 3, no. 2, pp. 021004/1–13, 2011.

[20] T. Morizono, K. Kurahashi, and S. Kawamura, "Analysis and control of a force display system driven by parallel wire mechanism," *Robotica*, vol. 16, no. 5, pp. 551–563, 1998.

[21] D. Surdilovic, J. Zhang, and R. Bernhardt, "STRING-MAN: Wire-robot technology for safe, flexible and human-friendly gait rehabilitation," in *Proc. IEEE Int. Conf. Rehabil. Robot.*, Noordwijk, The Netherlands, 2007, pp. 446–453.

[22] G. Rosati, P. Gallina, and S. Masiero, "Design, implementation and clinical tests of a wire-based robot for neurorehabilitation," *IEEE Trans. Neural Syst. Rehabil. Eng.*, vol. 15, no. 4, pp. 560–569, 2007.

[23] J.-P. Merlet and D. Daney, "A portable, modular parallel wire crane for rescue operations," in *Proc. IEEE Int. Conf. Robot. Autom.*, Anchorage, AK, 2010, pp. 2834–2839.

[24] M. Gobbi, G. Mastinu, and G. Previati, "A method for measuring the inertia properties of rigid bodies," *Mech. Syst. Signal Process.*, vol. 25, no. 1, pp. 305–318, 2011.
[25] M. Yamamoto, N. Yanai, and A. Mohri, "Trajectory control of incompletely restrained parallel-wire-suspended mechanism based on inverse dynamics," *IEEE Trans. Robot.*, vol. 20, no. 5, pp. 840–850, Oct. 2004.
[26] A. Fattah and S. K. Agrawal, "On the design of cable-suspended planar parallel robots," *ASME J. Mech. Des.*, vol. 127, no. 5, pp. 1021–1028, 2006.
[27] T. Heyden and C. Woernle, "Dynamics and flatness-based control of a kinematically undetermined cable suspension manipulator," *Multibody Syst. Dyn.*, vol. 16, no. 2, pp. 155–177, 2006.
[28] N. Michael, S. Kim, J. Fink, and V. Kumar, "Kinematics and statics of cooperative multi-robot aerial manipulation with cables," presented at the ASME Int. Des. Eng. Tech. Conf., vol. 7, San Diego, CA, 2009, pp. 83–91, Paper DETC2009–87677.
[29] Q. Jiang and V. Kumar, "The inverse kinematics of 3-D towing," in *Advances in Robot Kinematics: Motion in Man and Machine*, J. Lenarčič and M. M. Stanišic, Eds. Dordrecht, The Netherlands: Springer, 2010, pp. 321–328.
[30] Q. Jiang and V. Kumar, "The direct kinematics of objects suspended from cables," presented at the ASME Int. Des. Eng. Tech. Conf., vol. 2, Montreal, Canada, 2010, pp. 193–202, Paper DETC2010–28036.
[31] J.-F. Collard and P. Cardou, "Computing the lowest equilibrium pose of a cable-suspended rigid body," *Optim. Eng.*, 2012, DOI 10.1007/s11081–012–9191–5.
[32] M. Carricato and J.-P. Merlet, "Direct geometrico-static problem of under-constrained cable-driven parallel robots with three cables," in *Proc. IEEE Int. Conf. Robot. Autom.*, Shanghai, China, 2011, pp. 3011–3017.
[33] M. Carricato and J.-P. Merlet, "Inverse geometrico-static problem of under-constrained cable-driven parallel robots with three cables," presented at the 13th World Congr. Mech. Mach. Sci., Guanajuato, Mexico, 2011, pp. 1–10, Paper A7_283.
[34] M. Carricato, G. Abbasnejad, and D. Walter, "Inverse geometrico-static analysis of under-constrained cable-driven parallel robots with four cables," in *Latest Advances in Robot Kinematics*, J. Lenarčič and M. Husty, Eds. Dordrecht, The Netherlands: Springer, 2012, pp. 365–372.
[35] M. Carricato and G. Abbasnejad, "Direct geometrico-static analysis of under-constrained cable-driven parallel robots with 4 cables," in *Cable-Driven Parallel Robots*, T. Bruckmann and A. Pott, Eds. Dordrecht, The Netherlands: Springer, 2013, pp. 269–285.
[36] G. Abbasnejad and M. Carricato, "Real solutions of the direct geometrico-static problem of under-constrained cable-driven parallel robots with 3 cables: A numerical investigation," *Meccanica*, vol. 47, no. 7, pp. 1761–1773, 2012.
[37] A. Berti, J.-P. Merlet, and M. Carricato, "Solving the direct geometrico-static problem of 3-3 cable-driven parallel robots by interval analysis: Preliminary results," in *Cable-Driven Parallel Robots*, T. Bruckmann and A. Pott, Eds. Dordrecht, The Netherlands: Springer, 2012, pp. 251–268.
[38] D. T. Greenwood, *Advanced Dynamics*. Cambridge: Cambridge Univ. Press, 2006.
[39] D. G. Luenberger and Y. Ye, *Linear and Nonlinear Programming*. New York: Springer-Verlag, 2008.
[40] K. H. Hunt, *Kinematic Geometry of Mechanisms*. Oxford: Clarendon, 1978.
[41] D. Cox, J. Little, and D. O'Shea, *Ideals, Varieties, and Algorithms*. New York: Springer-Verlag, 2007.